Progranulin enhances the engraftment of transplanted human iPS cell-derived cerebral neurons

山上, 敬太郎

Progranulin enhances the engraftment of transplanted human iPS cell-derived cerebral neurons

Keitaro Yamagami, Bumpei Samata, Daisuke Doi, Ryosuke Tsuchimochi, Tetsuhiro Kikuchi, Naoya Amimoto, Megumi Ikeda, Koji Yoshimoto, Jun Takahashi

Stem Cells Translational Medicine, 2024, **13**, 1113–1128
https://doi.org/10.1093/stcltm/szae066
Advance access publication 28 September 2024
Original Research

Progranulin enhances the engraftment of transplanted human iPS cell-derived cerebral neurons

Keitaro Yamagami[1,2], Bumpei Samata[1], Daisuke Doi[1], Ryosuke Tsuchimochi[1,2], Tetsuhiro Kikuchi[1], Naoya Amimoto[1], Megumi Ikeda[1], Koji Yoshimoto[2], Jun Takahashi[*,1]

[1]Department of Clinical Application, Center for iPS Cell Research and Application, Kyoto University, Kyoto, Japan
[2]Department of Neurosurgery, Kyushu University Graduate School of Medical Sciences, Kyushu University, Fukuoka, Japan

[*]Corresponding author: Jun Takahashi, MD, PhD, Department of Clinical Application, Center for iPS Cell Research and Application, Kyoto University, 53 Shogoin-Kawahara-cho, Sakyo-ku, Kyoto 606-8507, Japan (jbtaka@cira.kyoto-u.ac.jp).

Abstract

Cerebral organoids (COs) in cell replacement therapy offer a viable approach to reconstructing neural circuits for individuals suffering from stroke or traumatic brain injuries. Successful transplantation relies on effective engraftment and neurite extension from the grafts. Earlier research has validated the effectiveness of delaying the transplantation procedure by 1 week. Here, we hypothesized that brain tissues 1 week following a traumatic brain injury possess a more favorable environment for cell transplantation when compared to immediately after injury. We performed a transcriptomic comparison to differentiate gene expression between these 2 temporal states. In controlled in vitro conditions, recombinant human progranulin (rhPGRN) bolstered the survival rate of dissociated neurons sourced from human induced pluripotent stem cell-derived COs (hiPSC-COs) under conditions of enhanced oxidative stress. This increase in viability was attributable to a reduction in apoptosis via Akt phosphorylation. In addition, rhPGRN pretreatment before in vivo transplantation experiments augmented the engraftment efficiency of hiPSC-COs considerably and facilitated neurite elongation along the host brain's corticospinal tracts. Subsequent histological assessments at 3 months post-transplantation revealed an elevated presence of graft-derived subcerebral projection neurons—crucial elements for reconstituting neural circuits—in the rhPGRN-treated group. These outcomes highlight the potential of PGRN as a neurotrophic factor suitable for incorporation into hiPSC-CO-based cell therapies.

Key words: hiPSC; organoids; progranulin; cell transplantation; transcriptome profiles; brain injuries.

Graphical abstract

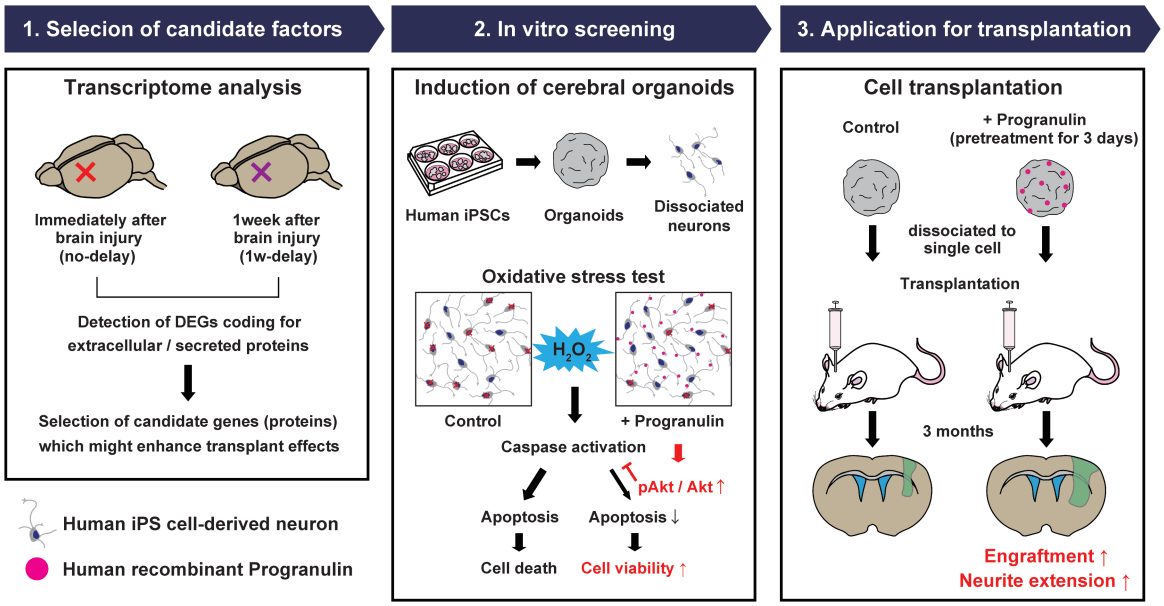

Received: 12 September 2023; Accepted: 12 July 2024.

Significance statement

The current study substantiates the potential benefits of administering recombinant human progranulin to induced pluripotent stem cell-derived cerebral organoids before transplantation. Specifically, progranulin significantly augmented both the engraftment process and the neurite extension along the corticospinal tracts in the host brains. This evidence supports an approach in which the therapeutic efficacy of cell transplants is enhanced by characterizing the host brain environment to identify and exploit potentially beneficial factors as exogenous neurotrophic stimulants before and after transplantation.

Introduction

Traumatic brain injury[1] or stroke,[2] due to damage to the cerebral motor cortex, often results in significant motor dysfunction and disabilities. Present treatment options, encompassing medication, surgeries, and rehabilitation, offer limited therapeutic effects stemming from the low regenerative potential of the central nervous system (CNS). As such, this necessitates the development of innovative treatment strategies to target fundamental recovery from brain damage. Cell replacement therapy emerges as a prospective alternative treatment, promising to restore the impaired neural circuits and facilitate functional recovery.[3,4] Earlier studies revealed that mouse embryonic brain tissues transplanted into the motor cortex formed long-distance efferent projections in the mature host brain, reconnected suitable cortical and subcortical host targets, and most notably, formed reciprocal synaptic connections with host tissues.[5,6] These findings affirm the potential application of cell transplantation therapy for damaged brains. Nevertheless, the application of embryonic tissues in humans is contentious due to ethical concerns.

A proposed remedy for this issue involves using cerebral organoids (COs), self-organizing 3D tissue cultures derived from pluripotent stem cells, which replicate the structure and physiology of the cerebrum and can serve as a renewable source of transplant material. A prior study reported that axonal extension along the corticospinal tract, a descending neuronal pathway from the cerebral cortex terminating at lower motor neurons or intermediate neurons in the spinal cord, was evident following the transplantation of human pluripotent stem cell (hiPSC)-derived COs into the cerebral cortices of mice.[7] Yet, acute post-transplantation cell death remains a prevalent issue for stroke, spinal cord injury, or other neurological disease models.[8] Thus, enhancements to the transplantation methodology, particularly concerning the engraftment of transplanted cells and subsequent neurite extension, are essential.

A multitude of strategies aiming to amplify the effects of transplants has been reported. One potential approach encompasses refining the host brain environment. Adeno-associated virus-mediated delivery of L1CAM, an axon guidance molecule, successfully promoted the axonal extension of grafted cells in a recent study.[9] In addition, an earlier report using viral delivery of glial cell line-derived neurotrophic factor (GDNF) to the host brain also showed encouraging results.[10] Given the adult brain's lower availability of neurotrophic or morphogenic proteins, crucial for cell survival, differentiation, and axonal connectivity compared to the developing brain,[10] another promising approach involves co-transplantation with growth factors. One study revealed that the viability and differentiation of transplanted neural stem cells and the protrusion of nerve fibers were significantly enhanced by co-transplantation with epidermal growth factor and basic fibroblast growth factor (bFGF).[11] However, validation studies concerning the benefits of neurotrophic factors on neural cell transplantation remain limited.

Peron et al[12] and Kitahara et al[7] demonstrated that transplantations undertaken a week post-injury significantly enhanced both engraftment and neuronal elongation compared to instances with no delay. The underlying mechanisms contributing to this phenomenon remain elusive, yet some potential contributors have been proposed. These include the release of neurotrophic and pro-angiogenic factors from cells in the area surrounding the injury and a reduction in both the inflammatory response and neurotoxic substances.[13] Accordingly, it was postulated that brain tissue assessed 1 week post-traumatic brain injury (1wpTBI) could provide a more conducive environment for cell transplantation when contrasted with immediate transplantations. Here, we performed a comparative transcriptome analysis to investigate the gene expression profiles between these 2 brain states. This approach established that progranulin (PGRN), a growth factor also known as granulin, epithelin precursor, or acrogranin,[14] markedly improved both engraftment and neurite elongation in hiPSC-COs in vitro and in vivo animal studies. Altogether, these findings underscore the potential of PGRN as a neurotrophic factor to be harnessed for cell transplantation therapy involving hiPSC-COs.

Material and Methods

Maintenance culture of human iPSCs

All experiments using hiPSCs were approved by the Ethics Committee of Kyoto University Graduate School and Faculty of Medicine. hiPSCs were maintained and cultured as previously described.[15] In brief, hiPSCs (S2WCB3) were maintained on a 6-well dish (MS-80060; Sumitomo Bakelite, Tokyo, Japan) coated with iMatrix-511 silk (MATRIXOME, Osaka, Japan) in StemFiT AK02N medium (Ajinomoto, Tokyo, Japan). When passaging the cells onto iMatrix-coated plates, iPSCs were dissociated into single cells with Cell Therapy Systems TrypLE Select CTS (Thermo Fisher Scientific, Waltham, MA, USA) containing 0.5 mmol/L-EDTA/PBS solution (Nacalai Tesque, Kyoto, Japan) and replated at a density between 1.0 and 2.0 × 10^4 cells per well with StemFit medium.

Differentiation culture of human iPSCs

Neuronal differentiation of human iPSCs was conducted using the serum-free floating culture of embryoid body-like aggregates with a quick reaggregation culture (SFEBq) method[7,16] with minor modification involving preconditioning. Several reports have reported the efficacy of pre-conditioning of iPSCs for the generation of organoids.[17-19] In brief, 1 day before inducting differentiation, the medium was changed to StemFiT AK02N medium (with components A and B but not component C) and 5 μM SB431542 (transforming growth factor β inhibitor; TOCRIS Bioscience, Bristol, UK). Several

lots of undifferentiated iPSCs were used to evaluate the efficacy of pretreatment, which generated organoids with more well structured, rosette-like structures (RLSs) compared to the conventional protocol (Supplementary Figure S1 A-C). On the day the SFEBq culture was started, hiPSCs were dissociated into single cells with Cell Therapy Systems TrypLE Select CTS (Thermo Fisher Scientific) containing 0.5 mmol/L-EDTA/PBS solution and 50 μM Y-27632 (Fujifilm Wako Pure Chemicals, Osaka, Japan), and quickly reaggregated using low-cell-adhesion-coated V-bottomed 96-well plates (PrimeSurface MS-9096V; Sumitomo Bakelite, Tokyo, Japan) in the differentiation medium (9000 cells/well, 100 μL) under 5% CO_2. The differentiation medium was DMEM/F12 with GlutaMAX (Thermo Fisher Scientific), supplemented with 20 % (vol/vol) Knockout Serum Replacement (Thermo Fisher Scientific, Waltham, MA, USA). Defining the day on which the SFEBq culture was started as day 0, 5 μM SB431542 (transforming growth factor β inhibitor; TOCRIS Bioscience, Bristol, UK; day −1 to day 18), 3 μM IWR1e (Wnt Inhibitor; Merck Millipore, Burlington, MA, USA; day 0 to day 18), and 50 μM Y-27632 (day 0 to day 3) were added to the culture. Culture medium (100 μL) was added on day 3. Medium change (120 μL removal and 80 μL addition on day 6; 70 μL removal and 80 μL addition on day 9 to day 15) was performed once every 3 days. At day 18, floating aggregates were transferred to 90-mm non-adhesive dishes (MS-1390R; Sumitomo Bakelite, Tokyo, Japan) and cultured further in suspension using a rotational culture system. After day 18, the differentiation medium was changed to DMEM/F-12 with GlutaMAX, supplemented with 1% (vol/vol) N-2 Supplement (Thermo Fisher Scientific), 1% (vol/vol) Chemically Defined Lipid Concentrate (Thermo Fisher Scientific), 0.25 μg/mL Amphotericin B (Thermo Fisher Scientific), 1% (vol/vol) penicillin-streptomycin (Thermo Fisher Scientific). Floating aggregates were cut into one-half or one-quarter with micro scissors under a stereo microscope between days 35 and 40 to avoid central necrosis. All medium was changed once every 3 days after day 18.

Neuronal dissociation culture

For dissociated neuronal cultures, neural cells were dissociated from iPSC-COs using a papain-containing Neuron Dissociation Solutions (291-78001; Fujifilm Wako Pure Chemicals, Osaka, Japan) on days 42-70 and plated onto plates coated with iMatrix-511 silk in DMEM Ham's/F12 (042-30795, Fujifilm Wako Pure Chemicals, Osaka, Japan) supplemented with 1% (vol/vol) L-glutamine (Thermo Fisher Scientific), 2% (vol/vol) B-27 supplement (Thermo Fisher Scientific), 1% (vol/vol) N-2 supplement, and 1% (vol/vol) penicillin-streptomycin.

Oxidative stress test and quantification of cell viability

Dissociated neurons derived from iPSC-COs were seeded at 4.0×10^4 cells in each well of a 96-well plate (92096, TPP, Schaffhausen, Switzerland) coated with iMatrix-511 silk and cultured at 37°C, 5% CO_2 in the same medium used for dissociation culture. The medium was removed 24 hours after seeding, and recombinant human proteins diluted in medium were added (100 μL/well). The concentrations of each recombinant human protein were as follows: apolipoprotein D, APOD (NBP1-99548; Novus Biologicals, Centennial, CO, USA), 250, 500 mg/dL; cathepsin D, Ctsd (1014-AS-010; R&D Systems, Minneapolis, MN, USA), 250, 500 mg/dL; cathepsin S, Ctss (1183-CY-010; R&D Systems, Minneapolis, MN, USA), 250, 500 mg/dL; lysozyme, LYZ (ab158839; abcam, Cambridge, UK), 250, 500 mg/dL; osteopontin, OPN (1433-OP-050 CF; R&D Systems, Minneapolis, MN, USA), 250, 500 mg/dL, progranulin, PGRN (2420-PG-050; R&D Systems, Minneapolis, MN, USA), 5, 10 μg/mL; secreted protein acidic and cysteine rich, SPARC (941-SP-050; R&D Systems, Minneapolis, MN, USA), 500, 1000 mg/dL. Hydrogen peroxide; H_2O_2 (Santoku Chemical Industries, Tokyo, Japan) diluted with medium (100 μL) was added to each well (the final concentration of H_2O_2 was 0.1 mM) and incubated at 37°C, 5% CO_2 for 24 hours. Dilution of H_2O_2 was made fresh from a 30% stock solution immediately before each experiment. Due to the highly reactive nature of H_2O_2 and its short half-life in diluted solution,[20] H_2O_2 was added within 3 minutes of dilution. Quantification of live cells was performed using alamarBlue Cell Viability Reagent (Thermo Fisher Scientific). The medium was replaced with medium containing 10% alamarBlue, and the fluorescence intensity (excitation 560 nm, emission 590 nm) was measured after incubating at 37°C, 5% CO_2 for 24 hours. Relative cell viability (% medium control) in each condition was calculated by dividing the signal intensity of each condition by that of the medium control (without oxidative stress).

Apoptosis assay using live cell imaging system

Dissociated neurons derived from iPSC-COs were seeded at 4.0×10^4 cells in each well of a 96-well plate coated with iMatrix-511 silk and cultured at 37°C, 5% CO_2 in the same medium used for the dissociation culture. The medium was removed 24 hours after seeding, and recombinant human PGRN (rhPGRN), diluted in medium (the final concentration of rhPGRN was 10 μg/mL), was added (100 μL/well). For apoptosis assay, Incucyte Caspase-3/7 Green Dye (4440; Essen BioScience, Inc., Ann Arbor, MI, USA) was added to each well (1:2000 in culture medium, for a final assay concentration of 2.5 μM). When added to the tissue culture medium, the inert non-fluorescent substrate enters cells, where activated caspase-3/7, if present, could cleave it to release a fluorescent DNA dye that stains the nuclear DNA. H_2O_2 diluted with medium (100 μL/well) was added to each well (the final concentration of H_2O_2 was 0.1 mM) and incubated at 37°C, 5% CO_2 for 12 hours. Phase-contrast microscopic images were automatically taken using the IncuCyte S3 Live Cell Imaging System (Essen Bioscience, Inc., Ann Arbor, MI, USA) immediately before and at 5 minutes, 3, 6, and 12 hours after the addition of H_2O_2. For inhibiting the PI3K-Akt signaling pathway, wortmannin (ab120148; abcam, Cambridge, UK) (10 μm) was added. Fluorescent objects were quantified as apoptotic cells using the Incucyte integrated analysis software. Cell viability was calculated as follows: $R = N - n/L$, where N is the number of dead cells in each image after exposure to H_2O_2, n is the number of dead cells in each image before exposure to H_2O_2, L is the the number of live cells in each image before exposure to H_2O_2.

Animals experiments

All animal experiments in this study were approved by the Institutional Animal Care and Use Committee of the Animal Research Facility at Kyoto University and conducted according to the Regulations on Animal Experimentation at Kyoto University. Animals were cared for and handled in

accordance with the Regulations on Animal Experimentation at Kyoto University. All mice had access ad libitum to standard mouse food and water and were housed under a 12-hour light/dark cycle for the duration of the study. Eighteen 11-week-old male mice (C57BL/6NCrSlc) were used for gene expression and Western blot analysis. Sixty 10-week-old SCID mice (male 30, female 30; C.B-17/IcrHsd-Prkdcscid) were used as recipients for hiPSC-CO transplantations. All mice were purchased from Shimizu Laboratory Supplies Company, Ltd. (Kyoto, Japan).

Pretreatment of cerebral organoids before transplantation

Three days before transplantation, rhPRGN and rhLYZ were added to the differentiation medium. The concentrations of rhPGRN and rhLYZ in the medium were 10 μg/mL and 500 ng/mL, respectively.

Surgical procedures for mice

All surgical procedures for mice were performed under anesthesia with intraperitoneal injection of a mixture of medetomidine hydrochloride (0.75 mg/kg), midazolam (4 mg/kg), and butorphanol (5 mg/kg). During the procedure, mice were clamped using a stereotaxic apparatus (Narishige, Tokyo, Japan) to maintain their heads in the horizontal position. For gene expression and Western blot analysis, 11-week-old male mice (C57BL/6NCrSlc) were anesthetized, and small midline skin incisions were made. Craniotomy (2 × 2 mm) over the motor cortex was performed using an electric drill (Minitor Co., Ltd., Tokyo, Japan) and a small cavity (0.5-2.5 mm rostral to the bregma, 0.5-2.5 mm lateral to the midline, and 1 mm in depth from the cortical surface) was made by aspirating the cortical tissue. After induction of euthanasia by cervical dislocation, whole brains were extracted immediately ($n = 4$) or 1 week after the lesion ($n = 4$). Whole brains were then transected using a brain slicer (Muromachi Kikai Co., Ltd., Tokyo, Japan), and brain tissues adjacent to the cavity with a 1.0-mm margin were collected. For transplantation, small midline skin incisions and a small craniectomy over the motor cortex (1.0 mm rostral to the bregma and from 2.0 mm lateral to the midline) were made using an electric drill. Six-week hiPSCs-COs were dissociated into single cells and suspended in the same medium used for dissociation culture supplemented with rhPGRN (10 μg/mL) and rhLYZ (500 ng/mL). After centrifugation, the supernatant was removed, with the cell pellet kept on ice until immediately before transplantation. A volume of 0.5 μL per site of cell pellet (approximately 2.0×10^5 cells) was injected using a stereotaxic apparatus (the injection speed was 0.5 μL/minute), targeting the frontal motor cortex (1.0 mm rostral to the bregma, 2.0 mm lateral to the midline, and 1.0 mm in depth from the cortical surface) using a sterile 22 G needle (Hamilton, Reno, NV, USA). After transplantation, the skin was sutured with 4-0 silk thread (NESCOSUTURE; alfresa, Osaka, Japan). The body temperature of mice was maintained in the normothermic range (37-38 °C) throughout the procedures with a feedback-controlled heating pad and incubator (Biomachinery Co., Ltd., Chiba, Japan).

Transcriptome analysis

Using the Cap Analysis Gene Expression (CAGE) method, we conducted gene expression analysis comparing 2 kinds of mouse brain tissue, immediate after injury and 1wpTBI. The CAGE method can be taken as a variation of RNA-seq, specialized in capturing the 5′ end of mRNAs at cap sites and identifying transcription start sites (TSSs).[21] By precisely defining TSSs, an RNA molecule generates only one tag per transcript in the CAGE method,[22] which provides an accurate high-throughput measurement of RNA expression.[23] We adopted the CAGE method in the present study for improved quantitative analysis. CAGE library preparation, sequencing, mapping, and gene expression and motif discovery analysis were performed by DNAFORM (Yokohama, Kanagawa, Japan), and the details of the method were described previously.[24] In brief, RNA quality was assessed by Bioanalyzer (Agilent) to ensure that RIN (RNA integrity number) is over 7.0 and A260/280 and 260/230 ratios were over 1.7. First-strand cDNAs were transcribed to the 5′ end of capped RNAs, attached to CAGE "barcode" tags, with sequenced CAGE tags mapped to the mouse mm9 genome using BWA software (version 0.5.9) after discarding ribosomal or non-A/C/G/T base-containing RNA sequences. For tag clustering, CAGE-tag 5′ coordinates were input for RECLU clustering, with the maximum irreproducible discovery rate and minimum count per million value both set to 0.1.

Statistical analysis

All statistical analyses were performed using a commercially available software package (GraphPad Prism 9; GraphPad Software, La Jolla, CA, USA). Statistical significance was tested with the Mann-Whitney test (unpaired, non-parametric) for 2-group comparisons, the Kruskal-Wallis test with Dunn's multiple-comparisons test (unpaired, non-parametric) for multiple-group comparisons, and the 2-way ANOVA with Tukey's or Sidak's multiple-comparisons test. Experimental data were expressed as means ± SD or mean ± SEM. Differences with $P < .05$ were considered statistically significant.

Results

Gene expression analysis unveiled candidate proteins to bolster engraftment

We have previously reported that 1-week-delayed transplantation after lesioning enhanced both CO engraftment and neurite extensions from the grafted cells along the host CST significantly.[7] These findings suggest that the brain environment at 1wpTBI is more conducive to transplantation and may provide additional support for grafted neurons compared to transplantation immediately after lesioning. Based on this hypothesis, the present study compared the gene expression profile between mouse brains of no-delay and 1wpTBI groups (Figure 1A) to discern novel factors that could potentiate the therapeutic impact of cell transplantation. Gene expression analysis for these brain tissues was based on CAGE (Cap Analysis of Gene Expression) transcriptomics, which led to the detection of 17 621 genes and the identification of 940 differentially expressed genes (DEGs). The full list of DEGs is shown in Supplementary Table S1 (GEO accession number: GSE269438). The established thresholds for DEGs were a log2 fold change (log2 FC) > 2 and a false discovery rate < 0.05. We then selected secreted proteins using secretomeP and performed a UniProt search to identify conserved human extracellular proteins among significantly upregulated genes (top 20) in 1wpTBI mouse brain tissues. Ultimately, 7 candidate genes were selected, all of which code

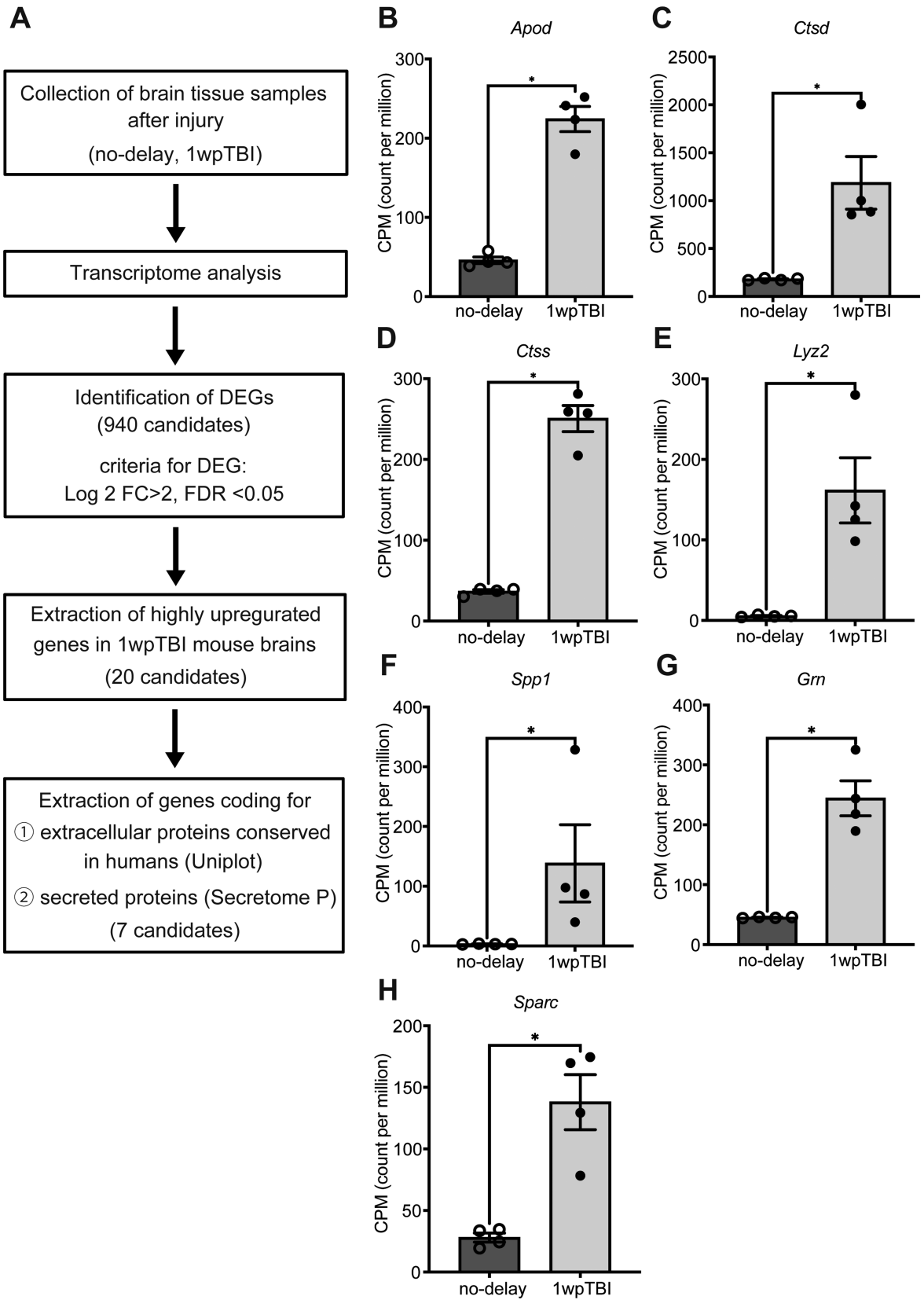

Figure 1. Gene expression analysis to identify candidate genes encoding novel host environment factors supporting grafted neurons. (A) Schematic flowchart describing the selection process of candidate genes. (B-H) Gene expression levels of the 7 candidate genes selected, as represented by count per million, for (B) *Apod*, (C) *Ctsd*, (D) *Ctss*, (E) *Lyz2*, (F) *Spp1*, (G) *Grn*, and (H) *Sparc*. Data are represented as the mean ± SEM, $n = 4$, Mann-Whitney test; $^*P < .05$.

for secreted and extracellular proteins (apolipoprotein D, *Apod*; cathepsin D, *Ctsd*; cathepsin S, *Ctss*; lysozyme 2, *Lyz2*; secreted phosphoprotein 1, *Spp1*; granulin, *Grn*; secreted protein acidic and cysteine rich, *Sparc*) (Figure 1B-H).

In vitro characterization of human iPSC-derived cerebral organoids

Next, the effects of these candidate proteins were evaluated using hiPSC-COs induced by our earlier protocol[7,16] with some modifications (Figure 2A). Six-week organoids contained RLSs (Figure 2B), primarily composed of neural progenitor cells expressing PAX6 and Ki67 (Figure 2C). Many deep-layer neurons (CTIP2$^+$) and a few upper-layer neurons (SATB2$^+$) were found surrounding these RLSs (Figure 2D and E). Cells positive for forebrain markers EMX1 and FOXG1 were found more extensively inside and outside the RLSs (Figure 2F and G).

Six-week organoids were dissociated into single cells and plated on laminin-coated 96-well plates to observe neurite extension from individual neurons (Figure 2H). Immunofluorescence experiments showed that dissociated neurons contained subcerebral projection neurons (SCPNs), which were positive for CTIP2 and Tuj1 (Figure 2I). On day 7, these SCPNs were interlinked by several neurites, indicating that the culture system effectively produced neural cells capable of forming neural circuits (Figure 2J).

Progranulin enhances the viability of dissociated neurons derived from cerebral organoids

To quantify the impact of the candidate proteins on neuronal cell survival, a cytotoxicity test with hydroxy peroxide (H_2O_2)—a reagent frequently used to induce oxidative stress—was performed. The percentage of live dissociated neurons was assessed following a 24-hour exposure to 0.1 mM H_2O_2. Whereas Alamar blue assays revealed that exogenous administration of recombinant human PGRN (rhPGRN) significantly enhanced neuronal viability (H_2O_2 0.1 mM, 50.3%; H_2O_2 0.1 mM + rhPGRN 10 µg/mL, 76.3%) (Figure 3A), other candidate proteins showed no substantial effects on cell survival. Next, to determine how rhPGRN augments cell survival, we performed time-lapse imaging with a fluorescent caspase-3/7-activated dye. rhPGRN (10 µg/mL) significantly reduced the percentage of caspase-3/7-positive cells after 6 to 12 hours of H_2O_2 exposure (Figure 3B and C). These results suggest that rhPGRN supports neuronal survival by mitigating apoptosis triggered by H_2O_2-induced oxidative stress. Based on these findings, rhPGRN was selected as a candidate protein for further investigation to protect transplanted cells.

Lysozyme promotes neurite extension from dissociated neurons

Dissociated neurons were plated on 96-well plates supplemented with the 7 candidate proteins separately to assess the impact of each candidate protein on neurite extension. Phase-contrast microscopy images were captured autonomously over 7 days using a live-cell imaging system. The quantification indicated that exogenous administration of recombinant human LYZ (rhLYZ) at concentrations of 500 ng/mL significantly promoted neurite outgrowth by the seventh day (control, 0.648 mm ± 0.038 mm; rhLYZ 500 ng/mL, 0.791 mm ± 0.039 mm) (Figure 4A). These beneficial effects of rhLYZ on neurite extension spanned from 24 to 168 hours post-seeding (Figure 4B and C). Conversely, the other candidate proteins showed no marked effects on neurite extension. Considering these findings, rhLYZ was identified as a candidate protein that could potentially boost the neurite extension of transplanted cells.

Progranulin enhances engraftment after transplantation of cerebral organoids in mice

Following the encouraging results of our in vitro experiments, the in vivo effects of rhPGRN and rhLYZ were evaluated for the transplantation of hiPSC-COs into 10-week-old SCID mice. The efficacy of these 2 proteins was augmented by a 3-day pretreatment of hiPSC-COs before transplantation (Figure 5A). Cellular composition within each preconditioned organoid was analyzed through flow cytometry by evaluating the percentages of neural (CTIP2, PAX6, and SATB2) and proliferation (Ki67) markers. There were no significant discrepancies in the percentages of cells expressing these markers between preconditioned groups (Figure 5B-E). Dissociated hiPSC-COs were implanted into the frontal motor cortex at specific coordinates (1.0 mm rostral to the bregma, 2.0 mm lateral to the midline, and 1.0 mm in depth from the cortical surface). Immunofluorescence experiments revealed successful cell engraftment and neurite extension originating from these engrafted cells at 3 months post-transplantation (Figure 5F). The survival rate of donor cells positive for the human-specific nucleic marker (Ku80 or hNuclei) was higher in the group treated with rhPGRN compared to the control group (Figure 5G). Next, we evaluated neural (CTIP2, PAX6, and SATB2) and proliferation (Ki67) markers in the grafts from each treatment group (Figure 5H). We found that the absolute number of graft-derived PAX6$^+$, CTIP2$^+$, SATB2$^+$, and Ki67$^+$ cells was significantly elevated in the rhPGRN-treated group compared to the control group (Figure 5I-L). Notably, except for CTIP2$^+$ cells in the rhPGRN-treated group, there were no significant differences between the treated and control groups when comparing the percentages of cells positive for those markers in the grafts (Figure 5M-P). In addition, we analyzed whether rhLYZ and rhPGRN treatment affected cell migration after transplantation. In the present study, we grafted iPSC-derived cortical neurons into the mouse cortex and found cell migration toward the ipsilateral striatum and not to other locations, such as the ipsilateral internal capsule, cerebral peduncle, or contralateral hemisphere. We further quantified the engrafted cell number in the cortex and ipsilateral striatum and observed no changes in Ku80-positive cells relative to the total number of grafted cells in either the cerebral cortex or striatum (Supplementary Figure S2A and B). These results showed that exogenous administration of rhPGRN nor rhLYZ alters the degree of cell migration after transplantation.

Progranulin enhances neurite extension along the corticospinal tract from the grafted cells in mice

Next, we examined the extension of graft-derived axons along the host corticospinal tract (CST) by immunostaining (Figure 6A) and quantified the human NCAM (hNCAM)-positive area. The rhPGRN-treated group exhibited a significantly larger hNCAM$^+$ area in the striatum, internal capsule, and cerebral peduncle compared to the control group (Figure 6B-D). To determine whether this enhancement in neurite extension was directly mediated by rhPGRN treatment or was an indirect effect of the increased number of grafted cells, we subsequently reevaluated the neurite extension data in each

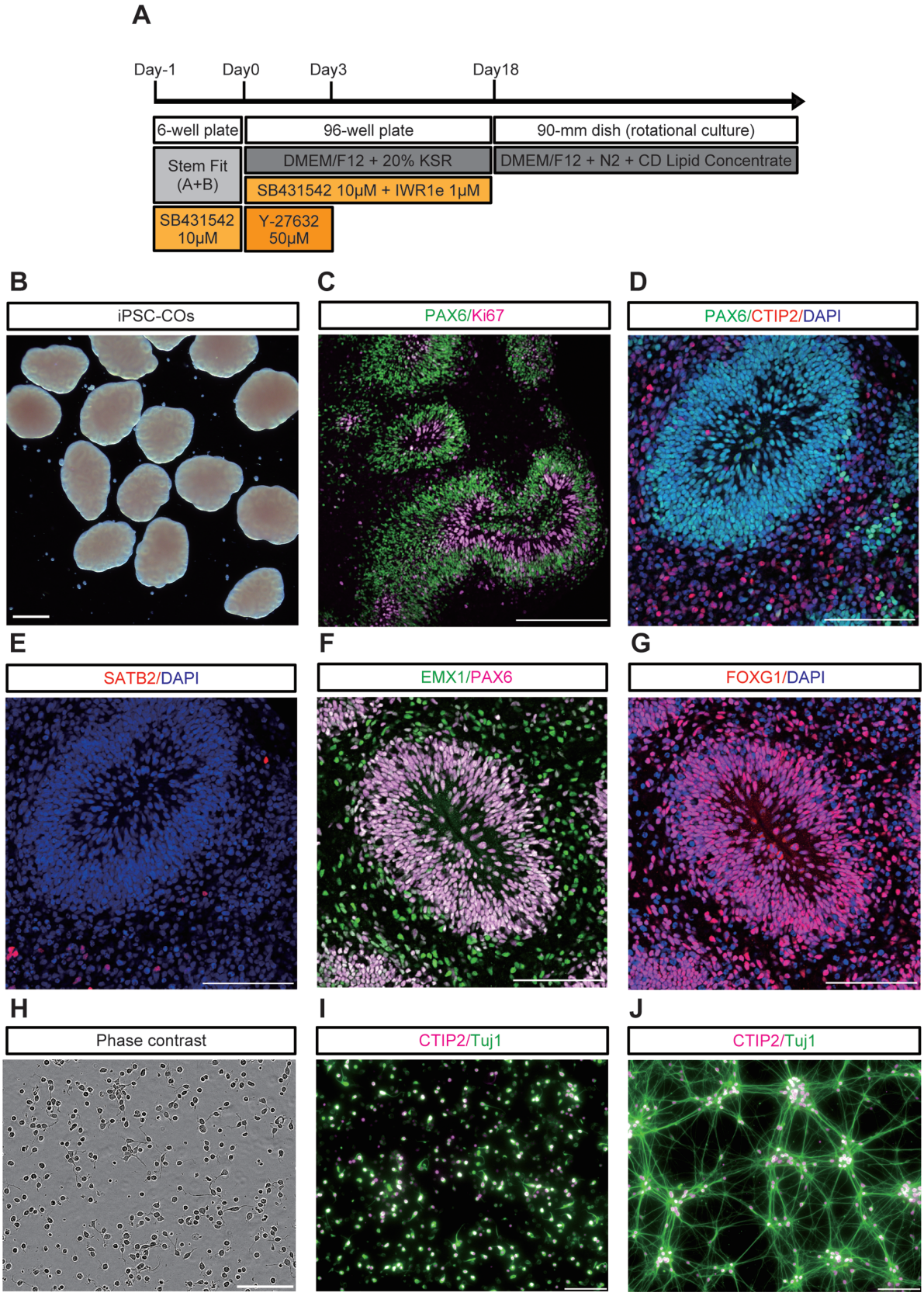

Figure 2. In vitro characterization of human iPSC-derived cerebral organoids and neuronal specification and maturation as dissociated neuronal cultures. (A) Schematic diagram of conditions for inducing cerebral organoids from hiPSCs. (B) Bright-field image of 6w-hiPSC-COs. Scale bar = 1 mm. Immunohistochemistry of 6w-hiPSC-COs. Immunofluorescence analysis for (C) PAX6 and Ki67, (D) PAX6 and CTIP2, (E) SATB2, (F) EMX1 and PAX6, (G) and FOXG1, with DAPI (nuclei). (H) Representative phase-contrast image of the dissociated neuronal culture of hiPSC-COs. Immunofluorescence analysis of dissociated neurons stained with CTIP2 and Tuj1 antibodies on (I) day 0 and (J) 7, respectively. Scale bars, 100 μm (C-H).

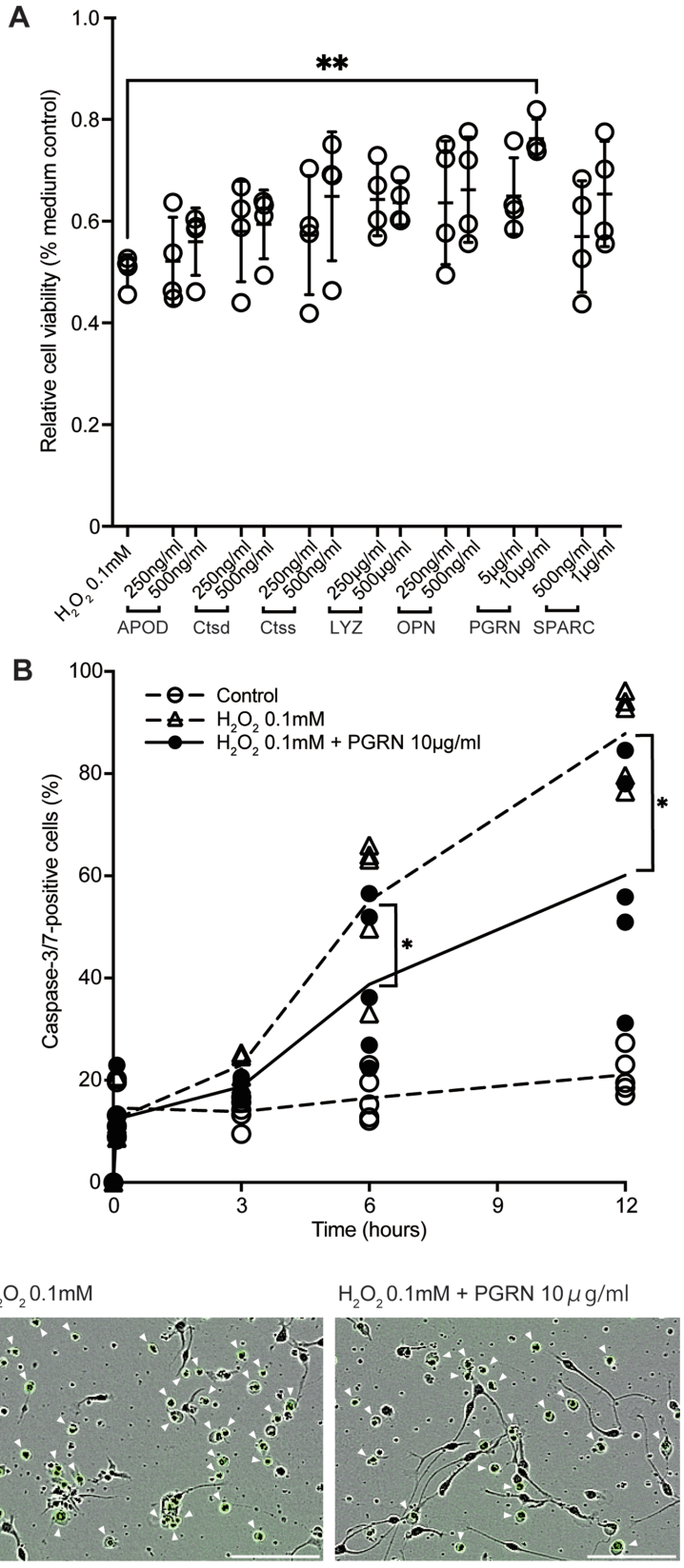

Figure 3. Progranulin enhanced the viability of dissociated neurons derived from cerebral organoids. (A) Relative cell viability (% medium control) under oxidative stress was measured by the alamarBlue assay. Data are represented as the mean ± SD, $n = 4$ independent experiments using quadruplicates for each group. Kruskal-Wallis test with Dunn's multiple comparisons test; ** $P < .01$. (B) Temporal change in the percentage of caspase-3/7-positive cells during oxidative stress as measured by live cell imaging system. The experiment was repeated 5 times using quadruplicates for each group. Two-way ANOVA with Dunnett's multiple comparisons test; *$P < .05$. (C) Representative phase-contrast images captured from live-cell imaging coupled with a fluorescent caspase-3/7-activated dye. Fluorescent green objects (white arrowheads) represent cells undergoing caspase-3/7-meditated apoptosis. Scale bars = 100 μm.

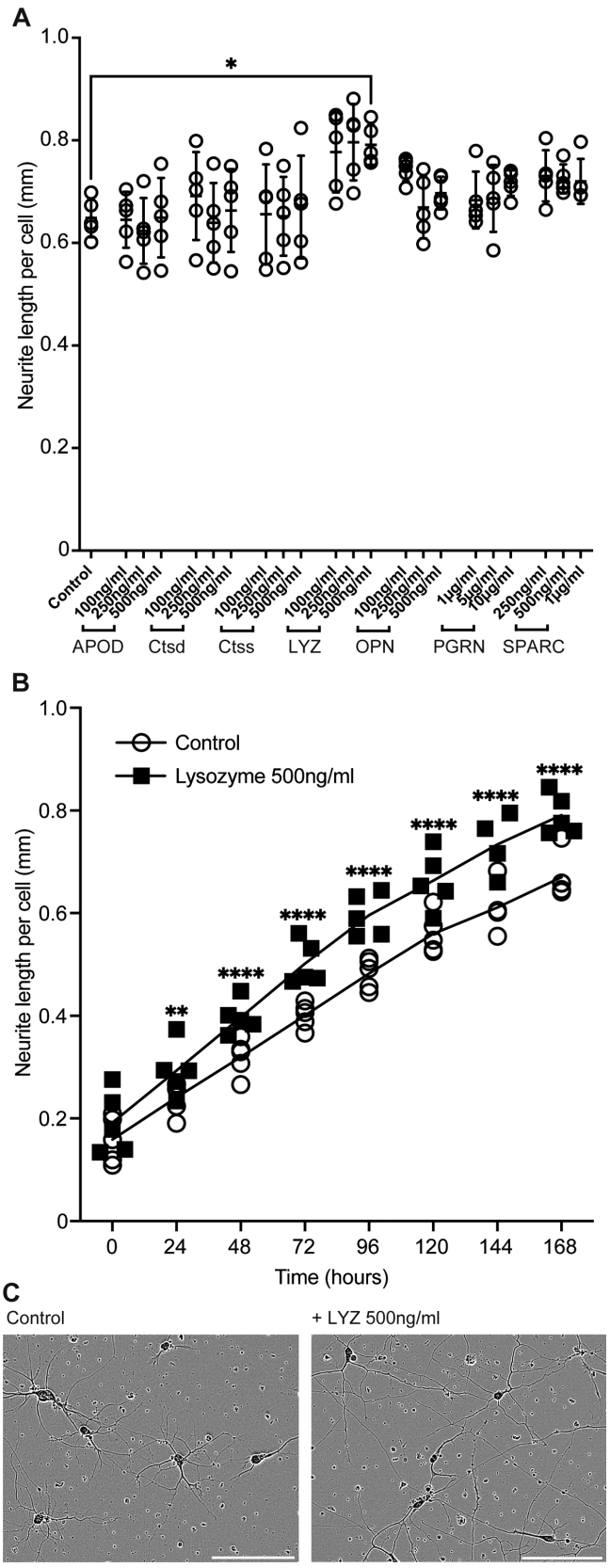

Figure 4. Lysozyme promoted neurite extension from dissociated neurons derived from cerebral organoids. (A) Neurite length per cell at day 7 in vitro was measured using a live-cell imaging system. Data are represented as the mean ± SD, $n = 5$ independent experiments using quadruplicates for each group. Kruskal-Wallis test with Dunn's multiple comparisons test; $^{*}P < .05$. (B) Time-dependent changes in the neurite length per cell during 168 hours (7 days) of culture. The experiment was repeated 5 times using quadruplicates for each group. Two-way ANOVA with Sidak's multiple comparisons test; $^{**}P < .01$ and $^{****}P < .0001$. (C) Representative phase-contrast images captured by live-cell imaging during dissociated neuronal culture with and without rhLYZ (500 ng/mL). Scale bars = 100 μm.

group by normalizing to the number of graft-derived CTIP2^{+} cells. Consequently, the positive effect of rhPGRN on neurite extension diminished after adjusting for the number of graft-derived CTIP2^{+} cells (Figure 6E-G). By contrast, although the beneficial effects on neurite extension by rhLYZ treatment were observed only in the striatum (Figure 6B), this enhancement remained even after adjusting for the number of graft-derived CTIP2^{+} cells (Figure 6E).

To confirm the axonal extension from the grafts, we retrograde-labeled the CST with a neuronal tracer 9 months post-transplantation in mice (Figure 6H). Briefly, we infused Fast Blue into the dorsal column of the spinal cord (contralateral to the transplantation site) 1 week before perfusion and examined for Ku80 and Fast Blue by immunofluorescence (Figure 6I). Notably, Ku80 (nucleus) and Fast Blue (cytoplasm) double-positive cells (Figure 6J-L) were observed in the rhPGRN-treated group (2 out of 3 mice, 66.7%), thus indicating graft cells had successfully extended axons down to their targets in the contralateral spinal cord. By contrast, no Ku80 and Fast Blue double-positive cells were observed in the control group (0 out of 3 mice, 0 %).

In summary, the 3-day pretreatment of hiPSC-COs by rhPGRN significantly promoted the engraftment of hiPSC-CO-derived neurons and neurite elongation to the striatum, internal capsule, and cerebral peduncle, in addition to increasing the proportion of CTIP2^{+} cells in the grafts. In contrast, rhLYZ did not significantly affect engraftment but promoted neurite elongation to the striatum.

Progranulin exhibited neuroprotection effects against oxidative stress by activating Akt cell signaling in dissociated neurons

Finally, we evaluated how PGRN enhanced neuronal survival. Before that, we performed Western blot analysis to confirm that PGRN increased not only at the gene expression level but also at the protein level in host brain tissues at 1wpTBI. We found that protein levels of PGRN increased in mouse brain tissues at 1wpTBI compared to those with no delay (Supplementary Figure S3A). To elucidate the mechanisms underpinning the neuroprotective effects of rhPGRN, the 2 prominent pro-survival cell signaling pathways known to mitigate oxidative stress[25] were investigated. To assess contributions by the PI3K/Akt pathway and the RAS-RAF-MEK-ERK (MAPK) pathway, we examined phosphorylated Akt (pAkt) and activated RAS following rhPGRN treatment. Intriguingly, quantitative analysis conducted through ELISA indicated a significant enhancement in AKT phosphorylation (pAkt/Akt) under the influence of rhPGRN (control, 0.3 ± 0.067; rhPGRN, 0.535 ± 0.22) (Figure 7A). By contrast, RAS activation displayed no substantial difference (Figure 7B). Next, to elucidate the relevance of the PI3/Akt pathway more strictly, co-treatment of wortmannin, a PI3-Akt inhibitor, with rhPGRN was performed. The rhPGRN-mediated neuroprotection effects under oxidative stress were inhibited by wortmannin (Figure 7C). This phenomenon was also confirmed in another iPS cell line (201B7) (Figure 7D). Altogether, these findings suggest that the neuroprotective

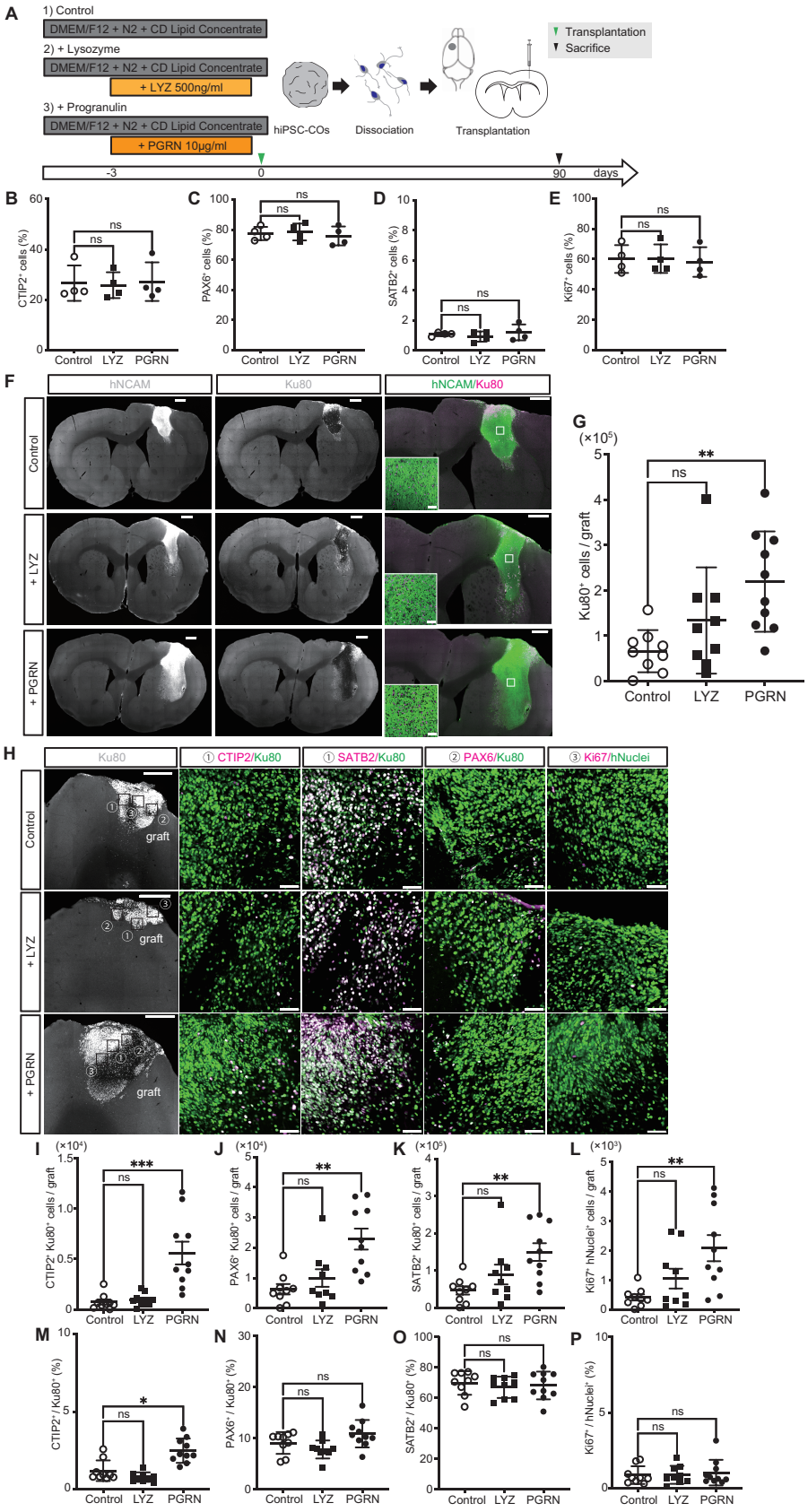

Figure 5. Progranulin enhanced engraftment after transplantation of cerebral organoids in mice. (A) Schematic overview of the cell transplantation. (B-E) Evaluation of the percentage of CTIP2-, PAX6-, SATB2-, and Ki67-positive cells contained within control, rhPGRN-treated, and rhLYZ-treated organoids by flow cytometry. Data are represented as the mean ± SD, $n = 4$ independent experiments. Kruskal-Wallis test with Dunn's multiple comparisons test. (F) Immunofluorescence analysis of hNCAM and Ku80. Insets show high-magnification images of the corresponding boxed areas. Scale bars = 500 μm (non-inset) and 50 μm (inset). (G) The number of Ku80-positive cells in the graft. Data are represented as the mean ± SD, $n = 9$ or 10, Kruskal-Wallis

effects of rhPGRN could be attributed to its ability to stimulate Akt cell signaling. Additionally, immunocytochemistry analysis was performed immediately after rhPGRN pretreatment to identify target cells of PGRN-induced Akt activation. Immunostaining showed that exogenously administered rhPGRN existed outside of the RLSs of COs and predominantly consisted of CTIP2$^+$ cells (Supplementary Figure 4A). Consistently, triple-staining for PAX6, CTIP2, and phospho-Akt (Ser473) revealed that Akt phosphorylation was enhanced by rhPGRN pretreatment only in CTIP2$^+$ cells (double positive for CTIP2 and phospho-Akt) but not PAX6$^+$ cells (Figure 7E and F). These results indicate that rhPGRN acts specifically on CTIP2$^+$ cells.

Discussion

This research aimed to systemically identify new factors capable of enhancing the efficacy of cell transplantation for neural circuit reconstruction with hiPSC-COs. We first used CAGE transcriptomics to ascertain host environmental factors advantageous for cell transplantation by comparing non-supportive and supportive brain environments (no-delay vs 1wpTBI) and, through a series of in vitro and mouse in vivo experiments, revealed that exogenous rhPGRN could significantly decrease intrinsic apoptosis by promoting neuronal viability against oxidative stress through activating the Akt pathway. By pretreating cells destined for transplantation with rhPGRN, significant increases in both the number of engrafted cells and neurite elongation were observed in our rodent model of acute traumatic brain injury, suggesting that rhPGRN could potentially act as a priming agent to reinforce engraftment and neurite elongation of iPSCs-derived cortical neurons for cell transplantation therapy.

This report is the first in the available literature demonstrating rhPGRN's efficacy in cell transplantation therapy. The findings from this study indicate a significant increase in grafted cells 3 months post-transplantation, attributable to exogenous rhPGRN. It also noticeably amplified neurite elongation along the corticospinal tract in our mouse model. However, the positive impact of rhPGRN on neurite elongation diminished after adjusting for the number of graft-derived CTIP2$^+$ cells. These observations imply that the noticeable neurite elongation resulted primarily from an indirect effect due to an augmented number of grafted cells rather than a direct effect mediated by rhPGRN.

PGRN, recognized as a pluripotent growth factor, is a secreted N-linked glycoprotein. It mediates various biological processes, including tissue regeneration, wound repair, inflammation, cell cycle progression, and tumorigenesis.[26] It is expressed in neurons and microglia within the central nervous system (CNS), playing critical roles in promoting neurite elongation, neuronal survival, and differentiation.[27,28] As a result, dysfunctional PGRN contributes to a myriad of neurological conditions. Mutations in *PGRN*, for instance, cause abnormal cleavage of TAR DNA binding protein-43 (TDP-43) by caspase-3 and lead to the accumulation of neurotoxic substances. This accumulation has been linked to neurodegenerative diseases, such as frontotemporal lobar degeneration with ubiquitin-positive inclusions (FTLD-Us) and amyotrophic lateral sclerosis.[29-31] Furthermore, a recent study demonstrated that human brain organoids with a loss of function in PGRN show TDP-43 mislocalization,[32] a common pathologic feature among the neurodegenerative diseases described above.

Previous in vitro research indicated that extracellular PGRN conferred protection to cortical neurons from oxidative stress triggered by H_2O_2.[27] The current study demonstrated that the exogenous introduction of rhPGRN protected against apoptosis and improved neuronal viability under oxidative stress induced by H_2O_2 in vitro. In addition, rhPGRN-mediated neuroprotective effects under oxidative stress were inhibited by wortmannin, a PI3-Akt inhibitor, thus implying that exogenous rhPGRN exerted antioxidant properties on cultured iPSC-derived cortical neurons. Consistently, previous literature reported that PGRN suppresses the production of reactive oxygen species from neutrophils by interfering with TNF signaling.[33]

It is widely recognized that 2 primary cell signaling pathways promote cell survival against oxidative stress: the PI3K/Akt and Ras-MAPK pathways.[25,34-36] Nonetheless, RAS activation, situated upstream of the MAPK pathway, was not observed in our experiments. Earlier studies posited that PGRN enhanced neuronal viability by triggering both the PI3/Akt and MAPK pathways.[27,37] In contrast, several studies claimed that PGRN exclusively activated the PI3/Akt pathway,[38,39] consistent with our results. Such discrepancies may be due to the inherent properties of cells examined, experimental methodologies, or the biological activity of PGRN used between different studies.

Another possible neuroprotective action of PGRN is the regulation of autophagy signaling.[40,41] PGRN deficiency resulted in autophagy impairment, causing pathological forms of TDP-43 to accumulate more rapidly in PGRN-deficient neurons, whereas administration of recombinant PGRN restored autophagy signaling. PRGN is also implicated in several processes maintaining normal function in the immune system in the CNS.[42] These findings imply that PGRN likely exerts its neuroprotective effect through multiple mechanisms.

Previous studies indicate that PGRN may contribute to neuroprotection and functional recovery following ischemic stroke[43-46] or traumatic brain injury.[47-49] Recent findings highlight a significant increase in PGRN protein levels in microglia between 3 and 14 days after an ischemic stroke that was released to inhibit neuronal ferroptosis.[46] Additionally, our data reveal that PGRN expression was considerably higher at 1wpTBI compared to non-delayed cases, consistent with a potential role for PGRN in tissue repair shortly after acute brain injury.

Considering these findings, PGRN could be a potential therapeutic agent for treating various acute brain injuries. A report indicated that the exogenous administration of rhPGRN, in conjunction with tissue plasminogen activators

test with Dunn's multiple comparisons test; $^{**}P < .01$. (H) Immunofluorescence analysis of Ku80, hNuclei, CTIP2, SATB2, PAX6, and Ki67 in the graft. The 4 columns on the right show high-magnification images of the boxed areas in the leftmost column and the number in the title of each magnified image corresponds to that of the boxed area. Scale bars = 500 μm (leftmost column) and 50 μm (other columns). (I-L) The number of graft-derived cells positive for CTIP2, PAX6, SATB2, and Ki67. Data are represented as the mean ± SEM, $n = 9$ or 10, Kruskal-Wallis test with Dunn's multiple comparisons test; $^{**}P < .01$ and $^{***}P < .001$. (M-P) Percentage of graft-derived cells expressing CTIP2, PAX6, SATB2, and Ki67. Data are represented as the mean ± SD, $n = 9$ or 10, Kruskal-Wallis test with Dunn's multiple comparisons test; $^{*}P < .05$.

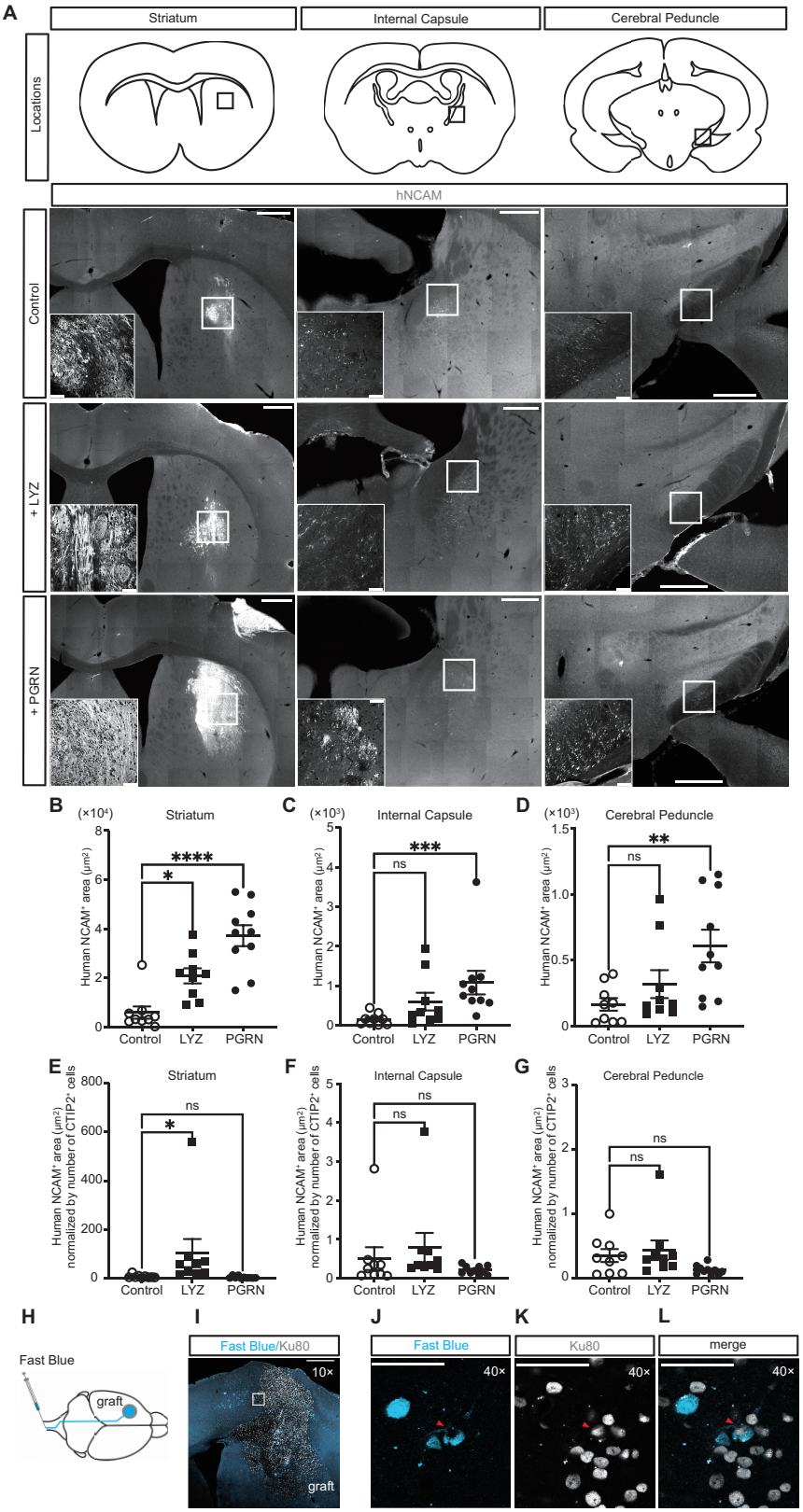

Figure 6. Progranulin enhanced neurite extension along the corticospinal tract from the grafted cells in mice. (A) Immunofluorescence analysis of hNCAM in representative brain sections. Insets show high-magnification images of the corresponding boxed areas. Scale bars = 500 μm (non-inset) and 50 μm (inset). Quantitative analysis of hNCAM-positive areas in each anatomical location: (B) striatum, (C) internal capsule, and (D) cerebral peduncle. Data are represented as the mean ± SEM, $n = 9$ or 10, Kruskal-Wallis test with Dunn's multiple comparisons test; $^{*}P < .05$, $^{**}P < .01$, $^{***}P < .001$, and $^{****}P < .0001$. Quantitative analysis of hNCAM-positive areas in each anatomical location adjusted by the number of CTIP2-positive cells in graft: (E) striatum, (F) internal capsule, and (G) cerebral peduncle. Data are represented as the mean ± SEM, $n = 9$ or 10, Kruskal-Wallis test with Dunn's multiple comparisons test; $^{*}P < .05$. (H) Schematic diagram of the procedures for retrograde labeling the corticospinal tract using Fast Blue. (I) Immunofluorescence analysis of Fast Blue and Ku80 in the graft. (J-L) Immunofluorescence analysis of Fast Blue and Ku80 in the higher magnification images of the corresponding boxed area in (I). Red arrowheads indicate a grafted cell labeled with Fast Blue. Scale bars = 500 μm (I) and 50 μm (J-L).

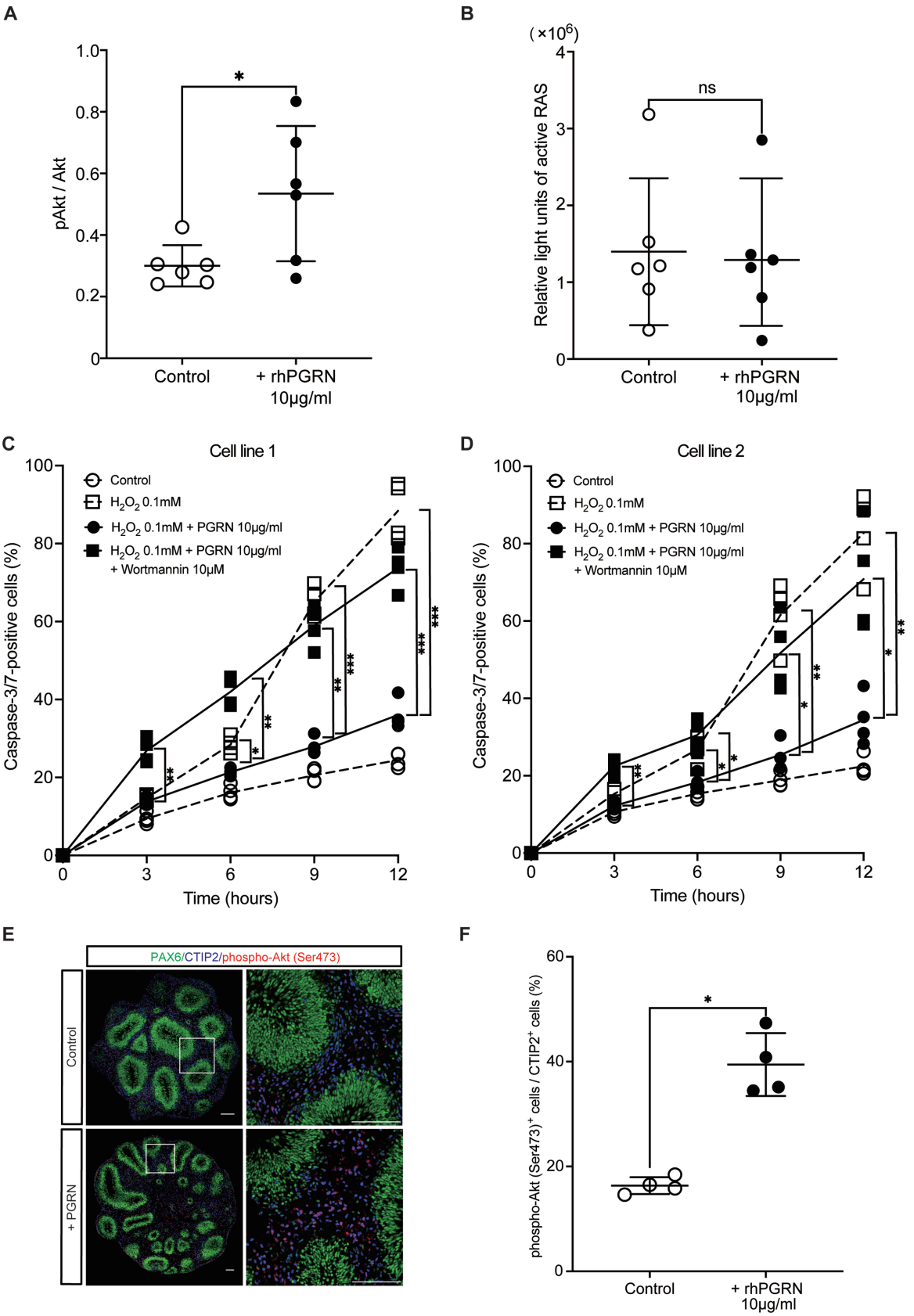

Figure 7. Progranulin exhibited neuroprotection effects against oxidative stress by activating Akt cell signaling in dissociated neurons derived from cerebral organoids. (A) Phosphorylation level of Akt (pAkt/Akt) as evaluated by ELISA. Data are represented as the mean ± SD, $n = 6$ independent experiments using duplicates for each group. Mann-Whitney test; $^*P < .05$. (B) Relative levels of activated RAS, as evaluated by ELISA. Data are represented as the mean ± SD, $n = 6$ independent experiments using duplicates for each group. Mann-Whitney test. Temporal change in the percentage of caspase-3/7-positive cells during oxidative stress with co-treatment of wortmannin, a PI3-Akt inhibitor, as measured by live cell imaging. (C) cell line

administered intravenously 4 hours post-middle cerebral artery occlusion (MCAO) in mice, resulted in a significant reduction in infarct volume, cerebral edema, hemorrhagic events, and mortality rates.[50] Concurrently, another study found that the intracerebroventricular administration of rhPGRN, initiated 30 minutes after MCAO, not only decreased infarct volume and functional deficits but also increased the count of proliferative cells in the subventricular zone 14 days post-ischemic injury.[37]

Despite the current lack of extensive knowledge on the efficacy of exogenous administration of PGRN for cell transplantation therapy, several factors have been identified as potential causes of donor cell death. These include mechanical stress, deprivation of growth factors, neuroinflammation, hypoxia, hypoxia-induced ER stress, and oxidative stress.[51,52] Our current data and prior studies[27,53] highlight the neuroprotective effects of rhPGRN against oxidative stress and hypoxia.[54] Given these findings, the administration of PGRN in cell transplantation therapy appears to be a logical step forward.

Notably, some reports describing the efficacy of recombinant PGRN on neurite outgrowth differed from our findings[28,55] and may be related to several factors. First, they used mouse or rat cells, whereas we used human cells, and species differences might have affected the results. Second, another possible reason is the method to measure the neurite length. While previous reports measured lengths of the longest neurite by immunostaining for neurofilament or phase-contrast images, we monitored the total neurite length per cell over 7 days using an automated live-cell imaging system. Furthermore, measurements were made 24 hours after seeding in those studies, thus much shorter than our observation, and comparisons were only between the control and PGRN-treated groups. Lastly, we conducted a one-way ANOVA analysis between the multiple condition groups. These differences in assessment methods and observation period after seeding might have affected the result.

This study used 6w-hiPSC-COs, primarily composed of cells positive for the neural progenitor marker PAX6 and the SCPN marker CTIP2. Our results showed that exogenously administered rhPGRN existed outside of PAX6$^+$ RLSs of COs, predominantly composed of CTIP2$^+$ cells. In addition, triple-staining for PAX6, CTIP2, and phospho-Akt (Ser473) revealed that Akt phosphorylation was observed only in CTIP2$^+$ cells but not PAX6$^+$ cells. These results indicate that rhPGRN acts specifically on CTIP2$^+$ cells. Considering these results, the relative increase of CTIP2$^+$ cells normalized to total graft cell number can be attributed to the protective effect of rhPGRN on CTIP2$^+$ cells rather than cell fate changes for PAX6$^+$ cells. Previous literature indicated that differentiated neurons tended to be extremely sensitive to altering external environments, such as physical stress and changes in temperature, pH, and osmolarity.[56] Another report also described postmitotic neurons as more vulnerable during dissociation and exhibited lower viability than neural precursor cells.[57] In this context, rhPGRN could act as a protective agent for these particularly vulnerable postmitotic neurons by activating Akt cell signaling.

In this study, rhLYZ emerged as another candidate protein, shown to enhance neurite elongation in dissociated neuronal cultures in vitro. Intriguingly, prior literature indicated a surge in the expression level of LYZ within activated microglia and macrophages following a complete spinal cord transection.[58] This increase potentially plays a role in providing neurotrophic support or promoting axonal regeneration. Although our in vivo experiments did not show an enhancement in the number of grafted cells with rhLYZ, they did reveal enhanced neurite elongation toward the striatum, which was still significant after adjusting for the number of CTIP2$^+$ cells, thus implying that the observable neurite extension resulted from a direct effect by rhLYZ on neurite outgrowth and/or extension. However, no substantial impact was observed beyond the striatum in more distant anatomical regions, such as IC or CP. Pretransplantation rhLYZ treatment may have been inadequate to facilitate continuous neurite elongation to these farther regions. As such, alternative treatment strategies designed to sustain a local therapeutic concentration—like a multiple-dose schedule or forced gene expression within the host brain via a viral vector—might be more effective.

This study has several limitations. First, hiPSCs-COs were transplanted into the intact mouse brains in the present study because we wanted to minimize the uncertain complexities of the host brain environment to evaluate the neurotrophic effects of rhPGRN discretely. As a next step, however, further investigation is indispensable to explore whether rhPGRN administration enhances engraftment and neurite elongation, even in stroke models or brain injury models. Secondly, although our data demonstrated that rhPGRN administration significantly enhanced neural cell survival and neurite elongation in vivo, we did not examine the graft-host neural connectivity or functional effects. The primary aim of this study was to identify novel trophic factors that enhance the viability of grafted neurons and promote neurite elongation; however, these issues should be addressed in future research. Thirdly, other options for administering rhPGRN should be examined. As mentioned earlier, pharmacological neuroprotective effects of PGRN via intravenous[50] or intraventricular[37] route have been reported, and such administration methods may be more applicable for clinical application. Finally, a more extended observation period (>3 months) after transplantation may be desirable to examine safety issues, such as tumorigenesis or graft overgrowth.

In summary, we established a supportive role of rhPGRN in hiPSC-CO transplantations through a comparative gene expression analysis between brain tissues at 1wpTBI and immediately following injury and a series of in vitro and in vivo experiments. These findings bolster the strategy in which the introduction of exogenous neurotrophic factors to mimic an optimal host environment enhances the therapeutic effects of cell transplantation.

Acknowledgments

We thank Sumitomo Pharma Ltd. for kindly providing cell lines; Ms. Kaori Fukushima, Ms. Rika Takaichi, and Ms.

1 (S2WCB3). (D) cell line 2 (201B7). The experiment was repeated 4 times using triplicate for each group. Two-way ANOVA with Dunnett's multiple comparisons test; *$P < .05$, **$P < .01$, and ***$P < .001$. Immunohistochemistry of 6w-hiPSC-COs. (E) Immunofluorescence analysis for PAX6, CTIP2, and phospho-Akt (Ser473). Scale bars = 100 μm. (F) Quantification for the percentage of CTIP2 and Ser473 double-positive cells within control and rhPGRN-treated organoids. Data are represented as the mean ± SD, $n = 4$ (n, number of aggregates). Kruskal-Wallis test with Dunn's multiple comparisons test; *$P < .05$.

Yuko Ishii for technical support with in vitro experiments; Mr. Naoya Amimoto for technical support with confocal laser microscopy; Mr. Kei Kubota for animal husbandry; Dr. Kelvin Hui for his critical reading of the manuscript; and all members of the Takahashi lab for their technical advice and insightful discussions.

Conflicts of Interest

The authors declared no potential conflicts of interest.

Data availability

The data reported in this article will be shared through reasonable requests to the corresponding author.

Funding

This work was supported by a grant from the Network Program for Realization of Regenerative Medicine from the Japan Agency for Medical Research and Development (AMED) (21bm0104001h0009 and 21bm0204004h0009) (to J.T.).

Author contributions

K.Y.: conception and design, collection and assembly of data, data analysis and interpretation, manuscript writing, and final approval of manuscript. B.S.: conception and design, collection and assembly of data, data analysis and interpretation, and final approval of manuscript. D.D.: provision of study material, collection of data, data analysis and interpretation, and final approval of manuscript. R.T., T.K., N.A., M.I.: collection of data and final approval of manuscript. K. Yoshimoto: final approval of manuscript. J.T.: conception and design, financial support, administrative support, provision of study material, data analysis and interpretation, manuscript writing, and final approval of manuscript.

Supplementary material

Supplementary material is available at *Stem Cells Translational Medicine* online.

References

1. Roozenbeek B, Maas AIR, Menon DK. Changing patterns in the epidemiology of traumatic brain injury. *Nat Rev Neurol*. 2013;9(4):231-236. https://doi.org/10.1038/nrneurol.2013.22
2. Yu Q, Yin D, Kaiser M, et al. Pathway-specific mediation effect between structure, function, and motor impairment after subcortical stroke. *Neurology*. 2023;100(6):616-626.
3. Grade S, Götz M. Neuronal replacement therapy: previous achievements and challenges ahead. *NPJ Regen Med*. 2017;2:29. https://doi.org/10.1038/s41536-017-0033-0
4. Jgamadze D, Lim JT, Zhang Z, et al. Structural and functional integration. of human forebrain organoids with the injured adult rat visual system. *Cell Stem Cell*. 2023;30(2):137-152.e7. https://doi.org/10.1016/j.stem.2023.01.004
5. Gaillard A, Prestoz L, Dumartin B, et al. Reestablishment of damaged. adult motor pathways by grafted embryonic cortical neurons. *Nat Neurosci*. 2007;10(10):1294-1299. https://doi.org/10.1038/nn1970
6. Ballout N, Frappé I, Péron S, et al. Development and maturation of embryonic cortical neurons grafted into the damaged adult motor cortex. *Front Neural Circuits*. 2016;10:55. https://doi.org/10.3389/fncir.2016.00055
7. Kitahara T, Sakaguchi H, Morizane A, et al. Axonal extensions along. corticospinal tracts from transplanted human cerebral organoids. *Stem Cell Rep*. 2020;15(2):467-481. https://doi.org/10.1016/j.stemcr.2020.06.016
8. David BT, Curtin JJ, Brown JL, et al. Temporary induction of hypoxic adaptations by preconditioning fails to enhance Schwann cell transplant survival after spinal cord injury. *Glia*. 2023;71(3):648-666. https://doi.org/10.1002/glia.24302
9. Tsuchimochi R, Yamagami K, Kubo N, et al. Viral delivery of L1CAM. promotes axonal extensions by embryonic cerebral grafts in mouse brain. *Stem Cell Rep*. 2023;18(4):899-914. https://doi.org/10.1016/j.stemcr.2023.02.012
10. Gantner CW, de Luzy IR, Kauhausen JA, et al. Viral delivery of GDNF promotes functional integration of human stem cell grafts in Parkinson's disease. *Cell Stem Cell*. 2022;26(4):511-526. http://doi.org/10.1016/j.stem.2020.01.010
11. Li H, Gan X, Pan L, et al. EGF/bFGF promotes survival, migration and. differentiation into neurons of GFP-labeled rhesus monkey neural stem cells xenografted into the rat brain. *Biochem Biophys Res Commun*. 2022;620:76-82. https://doi.org/10.1016/j.bbrc.2022.06.077
12. Péron S, Droguerre M, Debarbieux F, et al. A delay between motor cortex. lesions and neuronal transplantation enhances graft integration and improves repair and recovery. *J Neurosci*. 2017;37(7):1820-1834. https://doi.org/10.1523/JNEUROSCI.2936-16.2017
13. Ballout N, Rochelle T, Brot S, et al. Characterization of inflammation in. delayed cortical transplantation. *Front Mol Neurosci*. 2019;12:160. https://doi.org/10.3389/fnmol.2019.00160
14. He Z, Bateman A. Progranulin (granulin-epithelin precursor, PC-cell-derived growth factor, acrogranin) mediates tissue repair and tumorigenesis. *J Mol Med (Berl)*. 2003;81(10):600-612. https://doi.org/10.1007/s00109-003-0474-3
15. Adachi H, Morizane A, Torikoshi S, et al. Pretreatment with perlecan-conjugated laminin-e8 fragment enhances maturation of grafted dopaminergic progenitors in Parkinson's disease model. *Stem Cells Transl. Med.*. 2022;11(7):767-777. https://doi.org/10.1093/stcltm/szac033
16. Sakaguchi H, Ozaki Y, Ashida T, et al. Self-organized synchronous calcium transients in a cultured human neural network derived from cerebral organoids. *Stem Cell Rep*. 2019;13(3):458-473. https://doi.org/10.1016/j.stemcr.2019.05.029
17. Kuwahara A, Yamasaki S, Mandai M, et al. Preconditioning the initial state of feeder-free human pluripotent stem cells promotes self-formation of three-dimensional retinal tissue. *Sci Rep*. 2020;10(1):2237. https://doi.org/10.1038/s41598-020-58892-w
18. Shimada H, Sato Y, Sasaki T, et al. A next-generation iPSC-derived forebrain organoid. model of tauopathy with tau fibrils by AAV-mediated gene transfer. *Cell Rep Methods*. 2022;2(9):100289. https://doi.org/10.1016/j.crmeth.2022.100289
19. Ideno H, Imaizumi K, Shimada H, et al. Human PSCs determine the competency of cerebral organoid differentiation via FGF signaling and epigenetic mechanisms. *iScience*. 2022;25(10):105140. https://doi.org/10.1016/j.isci.2022.105140
20. Whittemore ER, Loo DT, Watt JA, Cotman CW. A detailed analysis of hydrogen peroxide-induced cell death in primary neuronal culture. *Neuroscience*. 1995;67(4):921-932. https://doi.org/10.1016/0306-4522(95)00108-u
21. Shiraki T, Kondo S, Katayama S, et al. Cap analysis gene expression for high-throughput analysis of transcriptional starting point and identification of promoter usage. *Proc Natl Acad Sci USA*. 2003;100(26):15776-15781. https://doi.org/10.1073/pnas.2136655100
22. Kanamori-Katayama M, Itoh M, Kawaji H, et al. Unamplified cap analysis of gene expression on a single-molecule sequencer. *Genome Res*. 2011;21(7):1150-1159. https://doi.org/10.1101/gr.115469.110
23. Takahashi H, Lassmann T, Murata M, Carninci P. 5′ end-centered expression profiling using cap-analysis gene expression and next-generation sequencing. *Nat Protocols*. 2012;7(3):542-561. https://doi.org/10.1038/nprot.2012.005

24. Ohmiya H, Vitezic M, Frith MC, et al; FANTOM Consortium. SOFTWARE Open Access RECLU: a pipeline to discover reproducible transcriptional start sites and their alternative regulation using capped analysis of gene expression (CAGE). *BMC Genomics*. 2014;15:269. https://doi.org/10.1186/1471-2164-15-269
25. Ong Q, Guo S, Duan L, et al. The timing of Raf/ERK and Akt activation in protecting PC12 cells against oxidative stress. *PLoS One*. 2016;11(4):e0153487. https://doi.org/10.1371/journal.pone.0153487
26. He Z, Ong CHP, Halper J, Bateman A. Progranulin is a mediator of the wound response. *Nat Med*. 2003;9(2):225-229. https://doi.org/10.1038/nm816
27. Xu J, Xilouri M, Bruban J, et al. Extracellular progranulin protects cortical neurons from toxic insults by activating survival signaling. *Neurobiol Aging*. 2011;32(12):2326.e5-2326.16. https://doi.org/10.1016/j.neurobiolaging.2011.06.017
28. Van Damme P, Van Hoecke A, Lambrechts D, et al. Progranulin functions as a neurotrophic factor to regulate neurite outgrowth and enhance neuronal survival. *J Cell Biol*. 2008;181(1):37-41. https://doi.org/10.1083/jcb.200712039
29. Zhang YJ, Xu YF, Dickey CA, et al. Progranulin mediates caspase-dependent cleavage of TAR DNA binding protein-43. *J Neurosci*. 2007;27(39):10530-10534. https://doi.org/10.1523/JNEUROSCI.3421-07.2007
30. Zhang Y-J, Xu Y-F, Cook C, et al. Aberrant cleavage of TDP-43 enhances aggregation and cellular toxicity. *Proc Natl Acad Sci USA*. 2009;106(18):7607-7612. https://doi.org/10.1073/pnas.0900688106
31. Pottier C, Zhou X, Perkerson RB, et al. Potential genetic modifiers of disease risk and age at onset in patients with frontotemporal lobar degeneration and GRN mutations: a genome-wide association study. *Lancet Neurol*. 2018;17(6):548-558. https://doi.org/10.1016/S1474-4422(18)30126-1
32. de Majo M, Koontz M, Marsan E, et al. Granulin loss of function in human mature brain organoids implicates astrocytes in TDP-43 pathology. *Stem Cell Rep*. 2023;18(3):706-719. https://doi.org/10.1016/j.stemcr.2023.01.012
33. Zhu J, Nathan C, Jin W, et al. Conversion of proepithelin to epithelins: roles of SLPI and elastase in host defense and wound repair. *Cell*. 2002;111(6):867-878. https://doi.org/10.1016/s0092-8674(02)01141-8
34. Wang X, McCullough KD, Franke TF, Holbrook NJ. Epidermal growth factor receptor-dependent Akt activation by oxidative stress enhances cell survival. *J Biol Chem*. 2000;275(19):14624-14631. https://doi.org/10.1074/jbc.275.19.14624
35. Salinas M, Diaz R, Abraham NG, Ruiz de Galarreta CM, Cuadrado A. Nerve growth factor protects against 6-hydroxydopamine-induced oxidative stress by increasing expression of heme oxygenase-1 in a phosphatidylinositol 3-kinase-dependent manner. *J Biol Chem*. 2003;278(16):13898-13904. https://doi.org/10.1074/jbc.M209164200
36. Jiang H, Zhang L, Koubi D, et al. Roles of Ras-Erk in apoptosis of PC12 cells induced by trophic factor withdrawal or oxidative stress. *J Mol Neurosci*. 2005;25(2):133-140. https://doi.org/10.1385/JMN:25:2:133
37. Liu Y, Ren J, Kang M, et al. Progranulin promotes functional recovery and neurogenesis in the subventricular zone of adult mice after cerebral ischemia. *Brain Res*. 2021;1757:147312. https://doi.org/10.1016/j.brainres.2021.147312
38. Kleinberger G, Wils H, Ponsaerts P, et al. Increased caspase activation and decreased TDP-43 solubility in progranulin knockout cortical cultures. *J Neurochem*. 2010;115(3):735-747. https://doi.org/10.1111/j.1471-4159.2010.06961.x
39. Alyahya AM, Al-Masri A, Hersi A, et al. The effects of progranulin in a rat model of acute myocardial ischemia/reperfusion are mediated by activation of the P13K/Akt signaling pathway. *Med Sci Monit Basic Res*. 2019;25:229-237. https://doi.org/10.12659/MSMBR.916258
40. Chang M, Srinivasan K, Freidman B, et al. Progranulin deficiency causes impairment of autophagy and TDP-43 accumulation. *J Exp Med*. 2017;214(9):2611-2618.
41. Elia L, Mason A, Alijiagic A, et al. Genetic regulation of neuronal progranulin reveals a critical role for the autophagy-lysosome pathway. *J Neurosci*. 2019;39(17):3332-3344.
42. Rhinn H, Tatton N, McCaughey S, Kurnellas M, Rosenthal A. Progranulin as a therapeutic target in neurodegenerative diseases. *Trends Pharmacol Sci*. 2022;43(8):641-652. https://doi.org/10.1016/j.tips.2021.11.015
43. Martens LH, Zhang J, Barmada SJ, et al. Progranulin deficiency promotes neuroinflammation and neuron loss following toxin-induced injury. *J Clin Invest*. 2012;122(11):3955-3959. https://doi.org/10.1172/JCI63113
44. Egashira Y, Suzuki Y, Azuma Y, et al. The growth factor progranulin attenuates neuronal injury induced by cerebral ischemia-reperfusion through the suppression of neutrophil recruitment. *J Neuroinflamm*. 2013;10:105. https://doi.org/10.1186/1742-2094-10-105
45. Jackman K, Kahles T, Lane D, et al. Progranulin deficiency promotes post-ischemic blood-brain barrier disruption. *J Neurosci*. 2013;33(50):19579-19589. https://doi.org/10.1523/JNEUROSCI.4318-13.2013
46. Chen T, Shi R, Suo Q, et al. Progranulin released from microglial lysosomes reduces neuronal ferroptosis after cerebral ischemia in mice. *J Cereb Blood Flow Metab*. 2023;43(4):505-517. https://doi.org/10.1177/0271678X221145090
47. Tanaka Y, Matsuwaki T, Yamanouchi K, Nishihara M. Exacerbated inflammatory responses related to activated microglia after traumatic brain injury in progranulin-deficient mice. *Neuroscience*. 2013;231:49-60. https://doi.org/10.1016/j.neuroscience.2012.11.032
48. Menzel L, Kleber L, Friedrich C, et al. Progranulin protects against exaggerated axonal injury and astrogliosis following traumatic brain injury. *Glia*. 2017;65(2):278-292. https://doi.org/10.1002/glia.23091
49. Zheng X, Mi T, Wang R, et al. Progranulin deficiency promotes persistent neuroinflammation and causes regional pathology in the hippocampus following traumatic brain injury. *Glia*. 2022;70(7):1317-1336. https://doi.org/10.1002/glia.24175
50. Kanazawa M, Kawamura K, Takahashi T, et al. Multiple therapeutic effects of progranulin on experimental acute ischaemic stroke. *Brain*. 2015;138(Pt 7):1932-1948. https://doi.org/10.1093/brain/awv079
51. Faleo G, Russ HA, Wisel S, et al. Mitigating ischemic injury of stem cell-derived insulin-producing cells after transplant. *Stem Cell Rep*. 2017;9(3):807-819. https://doi.org/10.1016/j.stemcr.2017.07.012
52. Rodríguez-Pallares J, García-Garrote M, Parga J, et al. Combined cell-based therapy strategies for the treatment of Parkinson's disease: Focus on mesenchymal stromal cells. *Neural Regen Res*. 2023;18(3):478-484.
53. Li X, Cheng S, Hu H, et al. Progranulin protects against cerebral ischemia-reperfusion (I/R) injury by inhibiting necroptosis and oxidative stress. *Biochem Biophys Res Commun*. 2020;521(3):569-576. https://doi.org/10.1016/j.bbrc.2019.09.111
54. Körtvelyessy P, Huchtemann T, Heinze HJ, Bittner DM. Progranulin and its related microRNAs after status epilepticus: possible mechanisms of neuroprotection. *Int J Mol Sci*. 2017;18(3):490. https://doi.org/10.3390/ijms18030490
55. Horinaka I, Hayashi H, Nagamoto T, et al. Effect of progranulin on proliferation and differentiation of neural stem/progenitor cells after oxygen/glucose deprivation. *Int J Mol Sci* . 2022;23(4):1949.
56. Karra D, Dahm R. Transfection techniques for neuronal cells. *J Neurosci*. 2010;30(18):6171-6177. https://doi.org/10.1523/JNEUROSCI.0183-10.2010
57. Martín-Ibáñez R, Guardia I, Pardo M, et al. Insights in spatio-temporal characterization of human fetal neural stem cells. *Exp Neurol*. 2017;291:20-35. https://doi.org/10.1016/j.expneurol.2017.01.011
58. Zhang KH, Xiao HS, Lu PH, et al. Differential gene expression after complete spinal cord transection in adult rats: An analysis focused on a subchronic post-injury stage. *Neuroscience*. 2004;128(2):375-388. https://doi.org/10.1016/j.neuroscience.2004.07.008